

# Effects of Operating Conditions on Stability of Gas-Phase Polyethylene Reactors

K. B. McAuley, D. A. Macdonald, and P. J. McLellan

Dept. of Chemical Engineering, Queen's University, Kingston, Ontario, Canada K7L 3N6

*Fluidized-bed polyethylene reactors are prone to unstable behavior and temperature oscillations (Choi and Ray, 1985b). Their work is extended to show the effects of ethylene feed system operation, reactor cooling system design, catalyst properties, and gas composition on reactor stability and dynamics. The analysis is performed using a well-mixed model, because heat- and mass-transfer resistances between multiple phases are small and are not required to account for the observed bifurcation phenomena. The addition of a gas recycle and heat exchanger system to the model significantly affects dynamic performance, including the formation of limit cycles. The size and dynamics of the heat exchanger, however, have little effect on the overall stability. In contrast, automation of the ethylene feed system to replace the monomer in the reactor as it is consumed leads to substantially different dynamic behavior than if the ethylene feed is maintained at a constant rate. Catalyst properties (multiple sites, activation energy, and deactivation) significantly affect dynamics and stability, whereas comonomer and other gases affect them only mildly. The results confirm that without proper temperature control, gas-phase polyethylene reactors are prone to instability, limit cycles, and excursions toward unacceptable high-temperature steady states.*

## Introduction

Polyethylene is the most popular of all synthetic commodity polymers, with current worldwide production of more than 30 billion tonnes per year. A large proportion of this polyethylene is produced in gas-phase reactors using Ziegler-Natta catalysts. One benefit of gas-phase polyethylene production is that there is no solvent present in the reactor system to be recovered and processed. Another advantage is that gas-phase processes usually operate at more moderate temperatures and pressures than high-pressure or liquid-phase polymerization systems. A disadvantage of gas-phase systems is that the temperature in the reaction zone must be maintained above the dew point of the reactants to avoid condensation and below the melting point of the polymer to prevent particle melting and agglomeration. Excellent reviews of industrial gas-phase polyethylene production technology have been provided by Choi and Ray (1985a) and Xie et al. (1994).

To ensure sufficient polymerization rates and maintain the temperature below the polymer melting point, commercial

gas-phase fluidized-bed polyethylene reactors are operated in a relatively narrow temperature range between 75 and 110°C (Xie et al., 1994). Even within this range, significant temperature excursions must be avoided because they can lead to low catalyst productivity and changes in product properties (McAuley and MacGregor, 1991, 1992, 1993). Past modeling studies (Choi and Ray, 1985b; McAuley, 1992) have indicated that gas-phase polyethylene reactors are prone to unstable behavior and temperature oscillations. The goal of this article is to extend this earlier work to show the effects of ethylene feed system operation and reactor cooling system parameters on the thermal behavior of the reactor. We also investigate the importance of catalyst deactivation and multiple catalyst sites, and show the effects of hydrogen, inert and comonomer concentrations on reactor stability and dynamics.

## Dynamics and Stability of Polymerization Reactors

Van Heerden (1953) was one of the first researchers to study the problems of multiple steady states and instability in chemical reactors. Later, Uppal et al. (1974, 1976) used bifur-

Correspondence concerning this article should be addressed to K. B. McAuley.

cation theory to study multiplicity and stability in their analysis of the autothermal CSTR problem. This seminal work prompted a rapid expansion in chemical reactor stability and multiplicity research in the late 1970s and early 1980s. Morbidelli et al. (1987) and Razon and Schmitz (1987) have provided excellent reviews of this research. Important new results on the application of singularity theory to determine the steady-state multiplicity patterns of different reactor configurations are still being developed (Lovo and Balakotaiah, 1992).

W. H. Ray and coworkers at the University of Wisconsin have performed a large portion of the multiplicity and stability research specific to polymerization reactors. In polymerization systems, multiplicity and oscillations can arise for a number of reasons, including particle nucleation and growth phenomena in emulsion polymerizations (Rawlings, 1985); gel effect (Jaisinghani and Ray, 1977; Schmidt and Ray, 1981; Schmidt et al., 1984; Adebekun et al., 1989); and autothermal effects (Hamer et al., 1981; Teymour and Ray, 1989, 1992a). The multiplicities and oscillations predicted for polyethylene reactors in the current article arise due to autothermal effects.

Teymour and Ray (1989, 1992a) have studied autothermal limit cycles and multiple steady states in the solution polymerization of vinyl acetate in a CSTR. A laboratory-scale polymerization reactor was used to validate their model and to confirm the existence of limit cycles and multiple steady states. Teymour and Ray (1992b) extended their model to demonstrate that the dynamics of full-scale industrial reactors can be even more complex than their lab-scale counterparts. For example, their full-scale model predicts period doubling bifurcations for the limit cycles and possibly even chaos, whereas these phenomena were not predicted at the laboratory scale. The difference in dynamics between small and large reactors results from the difference in volume to surface area. In lab-scale reactors, the heat capacity of the reactor walls and the rate of heat loss to the surroundings are relatively large and help to damp out temperature oscillations.

Feedback temperature controllers can often be used to stabilize reactors that are open-loop unstable. In their study of a full-scale polypropylene reactor Choi and Ray (1988) have shown that the steady-state operating point of industrial interest is almost always open-loop unstable. Without temperature control, the only stable steady states occur when the level in the reactor is controlled, but the reactor pressure is not. Pressure can only be controlled if a stabilizing feedback temperature controller is added to the system. Even though temperature control can be used to stabilize open-loop unstable systems, a good understanding of the underlying steady-state and transient behavior of the system is essential. This information is useful for designing control schemes, and for predicting and avoiding undesirable oscillations or runaway phenomena when the temperature controller fails or saturates.

Steady-state multiplicity in polyethylene reactors has been examined on two levels, at the small-scale of individual polymer particles, and at the macroscale of the whole reactor. Hutchinson and Ray (1987) modeled heat generation in and dissipation from particles in the fluidized bed and predicted multiple steady states for individual polymer particles. They showed that particle ignition and overheating leading to an

undesirable high temperature steady state can occur early in the lifetime of a polymer particle when the ratio of the mass of catalyst to the particle surface area is high. As the particles grow, their surface area increases and the catalyst decays, reducing the risk of particle melting. Hutchinson and Ray (1987) showed that particle overheating is largely unrelated to the efficiency of the macroscale heat removal system of the reactor. Even injection of liquid condensate onto the particles, which might occur when fluidized bed reactors are operated in condensed mode, has little or no effect on particle overheating (Hutchinson and Ray, 1991). Hence, the solution to the polymer particle ignition problem is one of proper catalyst design.

At the larger scale of the entire fluidized bed reactor, instability, multiple steady states, and limit cycles have been predicted using mechanistic models. In the very first article on the dynamics of polyethylene reactors, Choi and Ray (1985b) used a dynamic model accounting for separate bubble and emulsion phases in the bed to predict up to three steady states in a polyethylene reactor. Their analysis, which focused on the reactor alone without the associated heat exchanger, predicts that a Hopf bifurcation leads to oscillatory behavior. Talbot (1990) showed that a simplified back-mixed model also predicted multiple steady states. In simulations of ethylene/ $\alpha$ -olefin copolymerizations, McAuley (1992) used a well-mixed model to predict that gas-phase polyethylene reactors are prone to open-loop unstable behavior in operating regions of industrial interest, and showed that the system can be stabilized using a PID feedback controller.

In their dynamic analysis, Choi and Ray (1985b) used a comprehensive two-phase model that accounts for heat- and mass-transfer resistances between the emulsion and bubble phases in the fluidized bed. Recently, McAuley et al. (1994) compared steady-state predictions of a two-phase model and a simplified well-mixed model. They showed that temperature and concentration predictions of the two models differ by less than 2 or 3°C and 2%, respectively, in the operating range of industrial interest. Hence, at steady state, industrial fluidized-bed polyethylene reactors can be accurately modeled using a simplified well-mixed model.

The current article demonstrates that dynamic behavior and stability predictions from a simplified well-mixed model of the reactor are similar to those of Choi and Ray's two-phase model. As such, we used the simplified model for all subsequent analysis. First, the behavior of the reactor is analyzed on its own and it is shown that either one or three steady states is possible, depending on the catalyst feed rate. The local stability of the multiple steady states is analyzed to show that the low temperature steady state may be either stable or unstable. The middle steady state, however, is always unstable and the high temperature steady state is always stable. Next, a recycle stream and external cooler are added to the model, reflecting the usual industrial situation. We show that the behavior of the combined reactor and recycle system is very different from that of the reactor alone. There is a range of catalyst feed rates where no stable steady state exists, and within this range, limit cycle behavior is obtained.

The effects of adding an ethylene concentration controller to the combined reactor and recycle system are examined to demonstrate that the reactor feed system strategy can have a significant effect on stability and multiplicity. The effects of

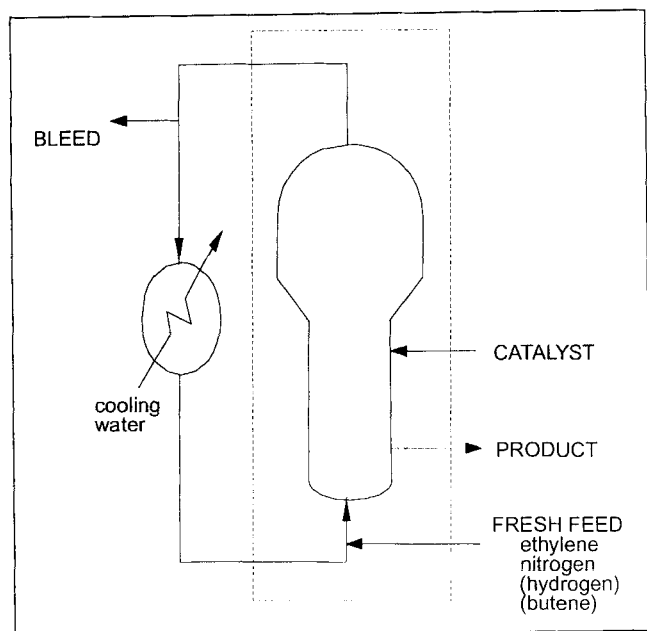


Figure 1. Gas-phase polyethylene reactor system.

heat exchanger dynamics and size are investigated, and are shown to have very little influence on the overall dynamics and stability of the system. In the original work of Choi and Ray (1985b), only ethylene homopolymerization was modeled using a nondeactivating single-site Ziegler-Natta catalyst. In the current article, we demonstrate the importance of catalyst deactivation and multiple catalyst sites, and investigate the effects of inerts, hydrogen, and comonomer to the reactor. We show that, while catalyst properties and the ethylene feed system have a significant influence, addition of comonomers and other gases to the reactor system have only a mild effect on multiplicity and stability.

### Single-Pass CSTR Model for the Fluidized Bed

A dynamic model of the polyethylene reactor shown within the dashed system boundary in Figure 1 can be derived by assuming that both the gas and the solid phases are well-mixed, that the temperature within the reactor is uniform, that the mass of polymer in the reactor is constant due to perfect bed-level control, and that there is only one type of catalyst site:

$$V_g \frac{d[M_1]}{dt} = F_{V1}([M_1]_0 - [M_1]) - R_{M1} \quad (1)$$

$$\frac{dY}{dt} = F_Y - k_d Y - Y \frac{O_p}{B_w} \quad (2)$$

$$(M_r C_{pr} + B_w C_{p\text{pol}}) \frac{dT}{dt} = H_0 - H_{\text{top}} + H_r - H_p \quad (3)$$

In the mass balance on the ethylene (Eq. 1),  $[M_1]$  is the concentration of ethylene in the reactor,  $V_g$  is the volume of the gas phase in the reactor,  $F_{V1}$  is the volumetric feed rate of the monomer to the reactor, and  $R_{M1}$  is the rate of ethylene

consumption due to reaction:

$$R_{M1} = [M_1] k_p(T) Y \quad (4)$$

where  $Y$  is the number of moles of catalyst sites in the reactor and  $k_p(T)$  is a temperature-dependent propagation rate constant:

$$k_p(T) = k_p(T_{\text{ref}}) \exp \left( \frac{-E_a}{R} \left( \frac{1}{T} - \frac{1}{T_{\text{ref}}} \right) \right) \quad (5)$$

where  $R$  is the ideal gas constant,  $E_a$  is the activation energy for propagation, and  $T_{\text{ref}}$  is a reference temperature at which the value of the rate constant is known.

In the catalyst mass balance (Eq. 2),  $F_Y$  is the molar feed rate of catalyst sites to the reactor that can be determined from the mass flow rate of catalyst to the reactor,  $F_c$ , and the active site concentration on the catalyst,  $a_c$ :

$$F_Y = F_c a_c \quad (6)$$

In Eq. 2,  $k_d$  is a deactivation rate constant,  $O_p = R_{M1} m_{w1}$  is the outflow rate of the polymer product from the reactor, and  $B_w$  is the mass of polymer in the bed. In the reactor energy balance (Eq. 3),  $T$  is the reactor temperature,  $M_r C_{pr}$  is the thermal capacitance of the reaction vessel, and  $C_{p\text{pol}}$  is the heat capacity of the polymer. The contribution of the gas to the heat capacity of the gas-phase reactor and its contents has been neglected.  $H_0$  is the enthalpy of the feed to the reactor and  $H_{\text{top}}$  is the enthalpy of gas leaving the reactor:

$$H_0 = F_{V1} [M_1]_0 C_{pg} (T_0 - T_{\text{ref}}) \quad (7)$$

$$H_{\text{top}} = F_{V1} [M_1] C_{pg} (T - T_{\text{ref}}) \quad (8)$$

$H_r$ , the rate of heat generation by reaction, is related to the enthalpy of reaction,  $\Delta H_R$  by

$$H_r = (-\Delta H_R) k_p(T) Y [M_1] m_{w1} \quad (9)$$

where  $m_{w1}$  is the molecular weight of ethylene.  $H_p$  is the enthalpy associated with the polymer leaving the reactor:

$$H_p = O_p C_{p\text{pol}} (T - T_{\text{ref}}) \quad (10)$$

In the development of the dynamic reactor model (Eqs. 1–3), it has also been assumed that the quantity of unreacted monomer leaving the reactor with the polymer is negligible. The rate of heat loss through the reactor wall is also neglected because it is much smaller than the other terms in Eq. 3.

Choi and Ray's (1985b) polyethylene reactor model, consisting of five differential equations, is more complicated than the current model because separate monomer and energy balances are required for the bubble and emulsion phases. The assumption of uniform monomer concentration and temperature in the gas (McAuley et al., 1994) leads to the current well-mixed model requiring only three differential equations.

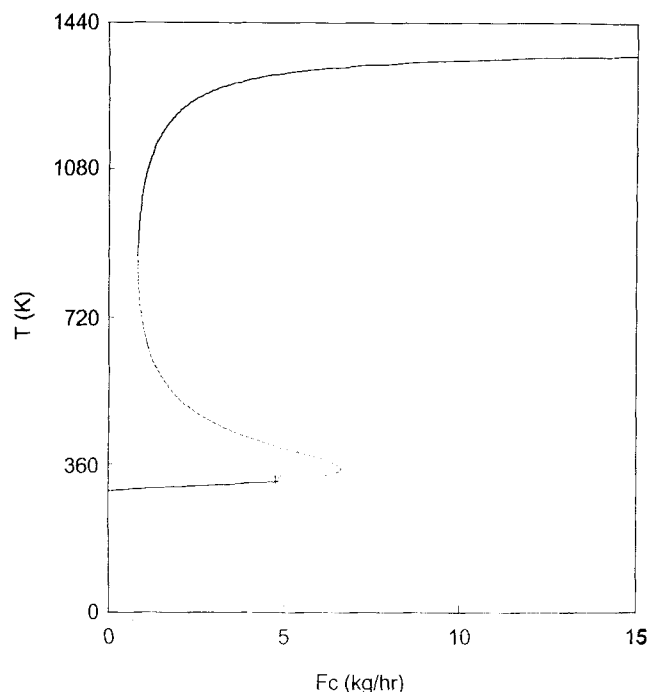


**Figure 2. Multiple steady states and stability for a single-pass gas-phase polyethylene reactor ( $k_d = 0$ ,  $E_a = 9,000$  cal/mol).**

—, Stable steady state; ---, unstable steady state; \*, Hopf bifurcation point.

The steady-state behavior predicted by the well-mixed model is shown in Figure 2, indicating that three possible steady states can occur for catalyst feed rates between 0.82 and 6.6 kg/h. For feed rates below 0.82 kg/h, only a single low temperature steady state exists and above 6.6 kg/h there is only a high temperature steady state. Since the melting point of polyethylene is approximately 400 K, the high temperature steady state predicted by the model would not actually be obtained. Instead the fluidized polymer particles would melt and agglomerate, and the well-mixed model would no longer be valid. The solid portions of the curve in Figure 2 indicate stable steady states, whereas the dashed portion is unstable. For catalyst feed rates greater than 4.7 kg/h, the lower portion of the steady-state curve is unstable. The instability arises at a Hopf bifurcation point which was determined using the AUTO software of Doedel (1986). Attempting to operate the reactor with a catalyst feed rate of 5 kg/h results in oscillation away from the low temperature unstable steady-state operating point and runaway toward the high temperature steady state. Therefore, feedback temperature control is required for safe operation of the reactor at catalyst feed rates beyond the Hopf bifurcation point.

The multiplicity and stability behavior shown in Figure 2 is very similar to that determined by Choi and Ray (1985b) using their two-phase model. It appears that a complicated model accounting for interactions between separate bubble and emulsion phases is not required to predict overall reactor dynamics and stability in the operating region of industrial interest, because resistances to heat and mass transfer between the two phases are small. McAuley et al. (1994) have

**Table 1. Reactor Operating Parameters Used in the Single-Pass Model**

$a_c$	0.548 mol/kg
$B_w$	70 tonne
$C_{pg}$	11.0 cal/(mol·K)
$C_{p, pol}$	0.85 cal/(g·K)
$E_a$	9,000 cal/mol
$F_{V1}$	28,000 L/s
$\Delta H_R$	894 cal/g
$k_d$	0 s <sup>-1</sup>
$k_p$ (360 K)	85 L/(mol·s)
$m_w$	28.05 g/mol
$[M_1]_0$	0.3 mol/L
$M_r C_{pr}$	14,000 kcal/K
$T_0$	298 K
$T_{ref}$	360 K
$V_g$	500 m <sup>3</sup>

shown that significant deviations between well-mixed and two-phase polyethylene reactor models can occur for high temperature reactor operation. Therefore, we expect our model predictions of steady-state operating temperatures will not be accurate for middle and high temperature steady-state portions of the curves. This is not a problem, however, because we are only interested in the portion of the steady-state operating curve that is below 400 K. The model parameters used to obtain Figure 2 are given in Table 1.

## Behavior of the Combined Reactor and Cooling System

### Mass balances

Most fluidized bed polyethylene reactors are cooled using a heat exchanger on the recycle gas line as shown in Figure 1. Since the single-pass conversion in these reactors is usually quite low (2–5%), the recycle stream is much larger than the fresh feed stream. Inert components and impurities are prevented from building up in the system by removing gas from the reactor, either along with the product or in a separate bleed stream. In the current model, we assume that a bleed stream is present, and that any gas exiting with the polymer is immediately captured and recycled to the reactor. We also neglect the short time-delay associated with the recycle gas flow through the heat exchanger and recycle lines, as well as any unreacted monomer or comonomer that leaves the reactor dissolved in the polymer particles. Using these assumptions, a dynamic ethylene mass balance can be written for the combined reactor and cooling system:

$$V_g \frac{d[M_1]}{dt} = F_{M1f} - b_{M1} - R_{M1} \quad (11)$$

where  $F_{M1f}$  is the molar feed rate of fresh ethylene to the reactor, and  $b_{M1}$  is the outflow rate of ethylene in the bleed stream. In some industrial ethylene polymerization systems, the time delay associated with transport of unreacted monomer through the recycle system and heat exchanger can be large, and can dominate the dynamics. This is especially true if the heat exchanger is used as a condenser or separator as in the BASF or AMOCO gas-phase processes (Xie et al., 1994). In the current article, only systems with negligible

**Table 2. Operating Parameters Used in the Combined Reactor and Heat Exchanger Model**

$AU$	$1.14 \times 10^6 \text{ cal}/(\text{s} \cdot \text{K})$
$C_{pH2}$	$7.7 \text{ cal}/(\text{mol} \cdot \text{K})$
$C_{pi}$	$6.9 \text{ cal}/(\text{mol} \cdot \text{K})$
$C_{pM1}$	$11.0 \text{ cal}/(\text{mol} \cdot \text{K})$
$C_{pM2}$	$24.0 \text{ cal}/(\text{mol} \cdot \text{K})$
$C_v$	$7.5 \text{ atm}^{-0.5} \cdot \text{mol/s}$
$F_R$	$8,500 \text{ mol/s}$
$F_{M1f0}$	$134 \text{ mol/s}$
$F_w C_{pw}$	$5.6 \times 10^6 \text{ cal}/(\text{s} \cdot \text{K})$
$K$	$5,737 \text{ mol}/(\text{atm} \cdot \text{s})$
$k_{f1}$	$0.088 \text{ L}/(\text{mol} \cdot \text{s})$
$k_{f2}$	$0.37 \text{ L}/(\text{mol} \cdot \text{s})$
$k_{h1}, k_{h2}$	$1.0 \text{ L}/(\text{mol} \cdot \text{s})$
$k_{p11} (360 \text{ K}), k_{p12} (360 \text{ K})$	$85 \text{ L}/(\text{mol} \cdot \text{s})$
$k_{p21} (360 \text{ K}), k_{p22} (360 \text{ K})$	$3 \text{ L}/(\text{mol} \cdot \text{s})$
$k_{r1}[R], k_{r2}[R]$	$4.0 \times 10^{-5}$
$m_{w1}$	$28.05 \text{ g/mol}$
$m_{w2}$	$56.2 \text{ g/mol}$
$p_{M1sp}$	$7.67 \text{ atm}$
$P_v$	$17 \text{ atm}$
$T_f$	$293 \text{ K}$
$T_w$	$293 \text{ K}$
$V_p$	$0.5$
$\tau$	$360 \text{ s}$
$\tau_I$	$1,500 \text{ s}$

monomer recycle time lags are considered. To control the ethylene pressure in response to changes in the ethylene consumption rate, the following PI control law has been implemented in most of the simulations in this article:

$$F_{M1f} = F_{M1f0} + K \left( e(t) + \frac{1}{\tau_I} \int e(t) dt \right) \quad (12)$$

where  $F_{M1f0}$  is the ethylene feed rate to the reactor when the controller is turned off, and  $e(t)$  is the error between the ethylene partial-pressure setpoint  $p_{M1sp}$  and the actual ethylene partial pressure, which can be determined from the ideal gas law:

$$p_{M1} = [M_1]RT. \quad (13)$$

Values for the tuning parameters,  $K$  and  $\tau_I$ , are given in Table 2. Simulations indicate that multiplicity and stability results are not very sensitive to the tuning of the ethylene partial-pressure controller.

The flow of ethylene in the bleed stream,  $b_{M1}$ , is equal to the mole fraction of ethylene in the gas-phase, multiplied by  $b$ , the total bleed stream flow rate that depends on the reactor pressure,  $P$ :

$$b = V_p C_v \sqrt{P - P_v} \quad (14)$$

where  $V_p$  and  $C_v$  are the bleed stream valve position and valve coefficient, respectively, and  $P_v$  is the pressure downstream of the bleed valve. Values for  $V_p$ ,  $C_v$ ,  $P_v$ , and all other parameters used to simulate the reactor behavior are given in Table 2.

Inert components such as nitrogen are added to gas-phase polyethylene reactors, either as a carrier for the catalyst, or

to help remove the heat of reaction from the polymer particles. Hydrogen is added to the reactor to control the molecular weight of the polymer. Butene or other comonomers can be added to control the density of the polymer (McAuley et al., 1990). The following mass balances can be written for these additional gas-phase components:

$$V_g \frac{d[I]}{dt} = F_{If} - b_I \quad (15)$$

$$V_g \frac{d[H_2]}{dt} = F_{H2f} - b_{H2} - R_{H2} \quad (16)$$

$$V_g \frac{d[M_2]}{dt} = F_{M2f} - b_{M2} - R_{M2} \quad (17)$$

where  $[I]$ ,  $[H_2]$ , and  $[M_2]$  are the concentrations of inerts, hydrogen, and comonomer, respectively, in the gas phase. The bleed flow rate of each component can be determined by multiplying the respective mole fraction by the total bleed rate. The rate of consumption of hydrogen by reaction,  $R_{H2}$ , is much smaller than the other terms in Eq. 16 and can be neglected.

Ziegler-Natta catalysts used for gas-phase ethylene polymerization can have multiple types of active sites, each with different rate constants and activation energies for propagation and deactivation reactions. The current model considers a two-site catalyst with temporary site deactivation due to chain transfer reactions with hydrogen (McAuley et al., 1990). The following mass balances can be written for each type of site:

$$\begin{aligned} \frac{dY_i}{dt} = & F_{Yi} - k_{di}Y_i - Y_i \frac{O_p}{B_w} - k_{fi}Y_i[H_2] + k_{ri}N_i[R] \\ & + k_{hi}N_i[M_1] \quad (i = 1, 2) \end{aligned} \quad (18)$$

where  $N_i$  is the number of moles of sites of type  $i$  deactivated by hydrogen;  $N_i$  can be obtained using the stationary state hypothesis

$$N_i = \frac{Y_i K_{fi}[H_2]}{k_{ri}[M_1] + k_{ri}[R] + O_{p/B_w}} \quad (i = 1, 2) \quad (19)$$

where  $k_{fi}$  is the rate constant for site deactivation by hydrogen, and  $k_{ri}$  and  $k_{hi}$  are rate constants for subsequent site reactivation reactions with cocatalyst and ethylene, respectively, and  $[R]$  is the concentration of cocatalyst in the reactor. Using this two-site catalyst, the rate of ethylene consumption is

$$R_{M1} = (k_{p11}Y_1 + k_{p12}Y_2)[M_1] \quad (20)$$

and the rate of butene consumption is

$$R_{M2} = (k_{p21}Y_1 + k_{p22}Y_2)[M_2] \quad (21)$$

where  $k_{pij}$  is a pseudopropagation rate constant for consumption of monomer  $i$  at catalyst sites of type  $j$ .

## Energy balances

Separate energy balances on the reactor and external heat exchanger are required to model the combined system. The reactor energy balance is similar to Eq. 3, except that the enthalpy of the gas stream entering the reactor is divided into two parts, the enthalpy of the fresh feed stream,  $H_f$ , and that of the recycle stream  $H_{g0}$ :

$$(M_r C_{pr} + B_w C_{pwl}) \frac{dT}{dt} = H_f + H_{g0} - H_{top} + H_r - H_p. \quad (22)$$

The enthalpy of the gas entering in the fresh feed stream,  $H_f$ , is

$$H_f = F_{M1f} C_{pgf} (T_f - T_{ref}), \quad (23)$$

and the enthalpy of the gas entering the reactor with the recycle stream is

$$H_{g0} = F_g C_{pg} (T_{g0} - T_{ref}). \quad (24)$$

The recycle flow rate,  $F_g$ , is controlled at a constant value by compressors on the recycle line to achieve good fluidization and mixing in the bed. The enthalpy of the gas leaving the reactor is

$$H_{top} = (F_g + b) C_{pg} (T - T_{ref}), \quad (25)$$

and  $H_p$ , the enthalpy associated with the polymer product stream, is given by Eq. 10.

The external heat exchanger has been modeled as a countercurrent single-pass exchanger with the recycle gas on the tube side and cooling water on the shell side. Steady-state analysis of such a system reveals that the gas-side outlet temperature is

$$T_{g0ss} = \frac{T_w \{1 - \exp(\gamma)\} - T \left\{1 - \frac{F_g C_{pg}}{F_w C_{pw}}\right\}}{\frac{F_g C_{pg}}{F_w C_{pw}} - \exp(\gamma)} \quad (26)$$

where

$$\gamma = AU \left( \frac{1}{F_g C_{pg}} + \frac{1}{F_w C_{pw}} \right) \quad (27)$$

where  $T_w$  is the cooling water inlet temperature,  $T$  is the temperature of the gas entering the heat exchanger,  $F_g$  and  $F_w$  are gas and cooling water flow rates,  $C_{pg}$  and  $C_{pw}$  are the respective heat capacities,  $A$  is the area available for heat transfer, and  $U$  is a heat-transfer coefficient.

To avoid using a complicated partial differential equation model for the dynamics of the shell and tube heat exchanger, the approach taken in the current study is to determine the steady-state heat-removal rate using Eq. 26, and then determine the dynamic heat-removal rate,  $Q_d$ , using a first-order approximation

$$\frac{dQ_d}{dt} = \frac{F_g C_{pg} (T - T_{g0ss}) - Q_d}{\tau} \quad (28)$$

where  $\tau$  is the first-order time constant for the exchanger. This approach gives only an approximate heat-removal rate from the system. However, the first-order approximation provides a more realistic method for predicting interactions between the reactor and external exchanger than that used by Choi and Ray (1985b), who assumed that the heat exchanger could instantaneously cool the recycle stream to a desired reactor inlet temperature. If Eq. 28 is used to predict the heat-removal rate in the exchanger, then the enthalpy of the recycle stream entering the reactor can be determined from

$$H_0 = H_{top} - H_b - Q_d \quad (29)$$

where  $H_b$ , which is the enthalpy associated with the bleed stream, is very small and can be neglected.

## Stability and Multiplicity Results for the Combined Reactor and Cooling System

### Constant ethylene feed policy

The steady-state reactor temperature obtained for different catalyst feed rates using a constant fresh ethylene feed rate of 134 mol/s is shown in Figure 3. A single-site catalyst

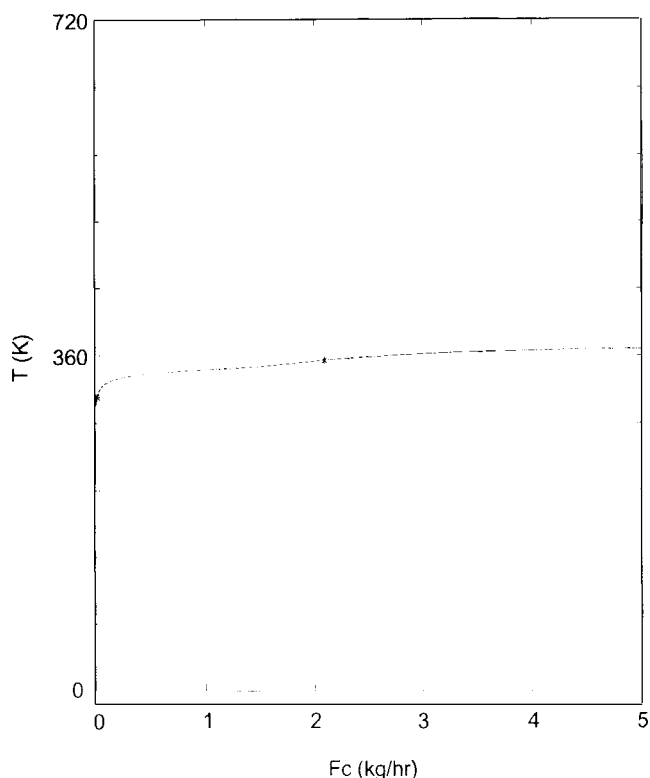


**Figure 3. Steady states and stability for the combined reactor and cooling system for a constant ethylene feed rate of 134 mol/s ( $k_d = 0.0001 \text{ s}^{-1}$ ,  $E_a = 9,000 \text{ cal/mol}$ ).**

—, Stable steady state; ---, unstable steady state; \*, Hopf bifurcation point.

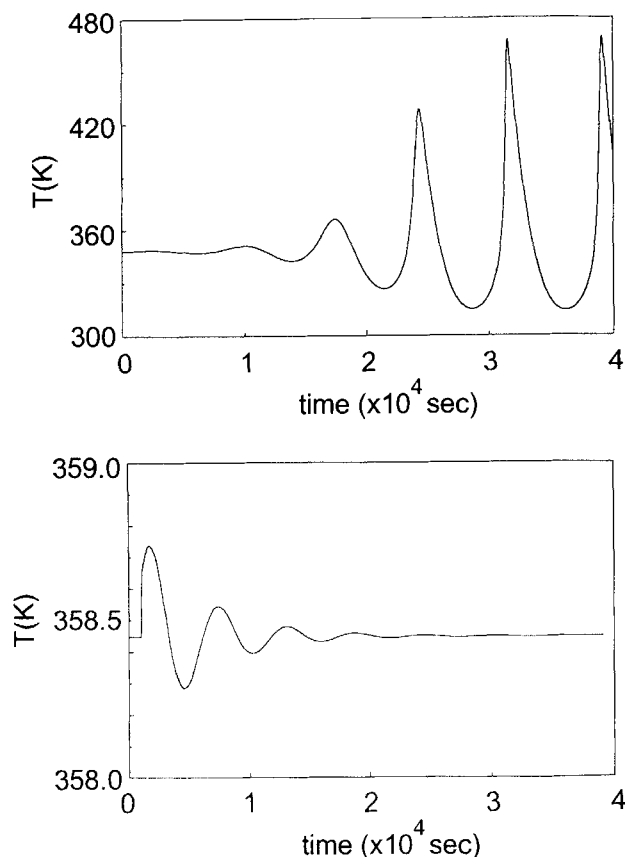


**Figure 4. Dynamic response of the reactor system to a cooling water temperature disturbance.**

(a)  $F_c = 1.5$  kg/h; (b)  $F_c = 2.5$  kg/h.

( $E_a = 9,000$  cal/mol,  $kd = 0.0001/\text{s}^{-1}$ ) is used in the analysis, ethylene is the only gas-phase reactant, and nitrogen is fed to the reactor at a rate of 2 mol/s. Notice that multiple steady states are not observed, and that unstable reactor behavior is predicted for catalyst feed rates between 0.03 and 2.1 kg/h. Figure 4a and b show the open-loop reactor behavior in response to a small cooling water temperature disturbance, for catalyst feed rates of 1.5 and 2.5 kg/h, respectively. In both simulations, the reactor operates at the unstable steady state for the first 1,000 s. At this time the cooling water temperature increases from 293 to 295 K and remains at the new level for 100 s before returning to 293 K. As predicted in Figure 3, reactor operation without a feedback temperature controller at a catalyst feed rate of 1.5 kg/h leads to unstable oscillatory behavior. Limit cycle behavior like that shown in Figure 4a, although predicted by the dynamic model, would not be observed in a gas-phase polyethylene reactor. Once the reactor temperature reached the melting point of the polymer particles ( $\sim 400$  K), agglomeration and loss of fluidization would occur rapidly, leading to reactor shutdown. The cooling water temperature disturbance has only a minor effect on the reactor temperature when the catalyst feed rate is 2.5 kg/h (Figure 4b). The reactor temperature increases by approximately 0.3 K, and then oscillates back to the original steady state.

The unstable steady states in Figure 3 and the limit cycles in Figure 4a can be explained mathematically by the presence

of Hopf bifurcation points, where complex conjugate pairs of eigenvalues of the Jacobian matrix for the dynamic model cross the imaginary axis. Physically, the oscillatory behavior can be explained by positive feedback between the reactor temperature and the reaction rate. If the reactor temperature is above the unstable steady-state temperature, then the heat-removal rate in the heat exchanger is larger than the steady-state heat-generation rate (McAuley, 1992). As a result, the reactor temperature begins to decrease, decreasing the rate of reaction. The product outflow rate from the reactor is reduced, thereby reducing the rate at which catalyst flows from the reactor with the polymer product. Thus, catalyst and monomer begin to accumulate in the reactor. When enough catalyst and monomer have accumulated, the rate of reaction begins to increase, increasing the reactor temperature and the product outflow rate. When the monomer concentration is very low and most of the catalyst has left the reactor in the product outflow stream, the reaction rate and reactor temperature begin to fall, and the cycle begins again. This type of unstable oscillatory behavior does not occur for higher catalyst feed rates, as in Figure 4b, where the reactor operates in a monomer-starved mode. Sufficient catalyst is present in the reactor at all times so that the concentration of ethylene in the system remains very low. Such low ethylene concentrations are not observed in industrial polyethylene reactors because the ethylene pressure in the reactor is maintained using a feedback controller that manipulates the fresh ethylene feed rate. As demonstrated in the next section, the presence of an ethylene pressure controller can lead to multiple steady states and higher operating temperatures because the controller ensures that there is always a ready supply of ethylene in the reactor.

#### **Reactor operation using an ethylene partial-pressure controller**

Addition of an ethylene partial-pressure controller (Eq. 12) to the system has a significant effect on multiplicity and stability. As ethylene is consumed by the reaction, the controller increases its feed rate to maintain the ethylene partial pressure at the desired setpoint. The stability and multiplicity behavior for the reactor system is shown in Figure 5 for ethylene partial-pressure setpoints of 3, 7.67, and 15 atm. Either one or three steady states is possible, depending on the ethylene partial-pressure setpoint and on the catalyst feed rate. Figure 5 illustrates that high ethylene concentrations in the reactor make the system more prone to runaway to unacceptable high temperature steady states. At an ethylene pressure of 15 atm, the lower steady-state branch exists only for catalyst feed rates up to 4.8 kg/h, whereas for an ethylene pressure of 3 atm, the lower steady-state branch extends to a catalyst feed rate of 14.6 kg/h.

Figure 6 shows the effect of the activation energy of the catalyst on stability and multiplicity for reactor operation at an ethylene pressure setpoint of 7.67 atm. All of the catalysts shown in Figure 6 have the same propagation rate constant at 360 K, but exhibit different activation energies. For a catalyst with a low activation energy (5,000 cal/mol), single stable steady states are observed for a given catalyst feed rate. Increasing the catalyst feed rate results in a monotonic increase in the steady-state temperature, and can result in operating

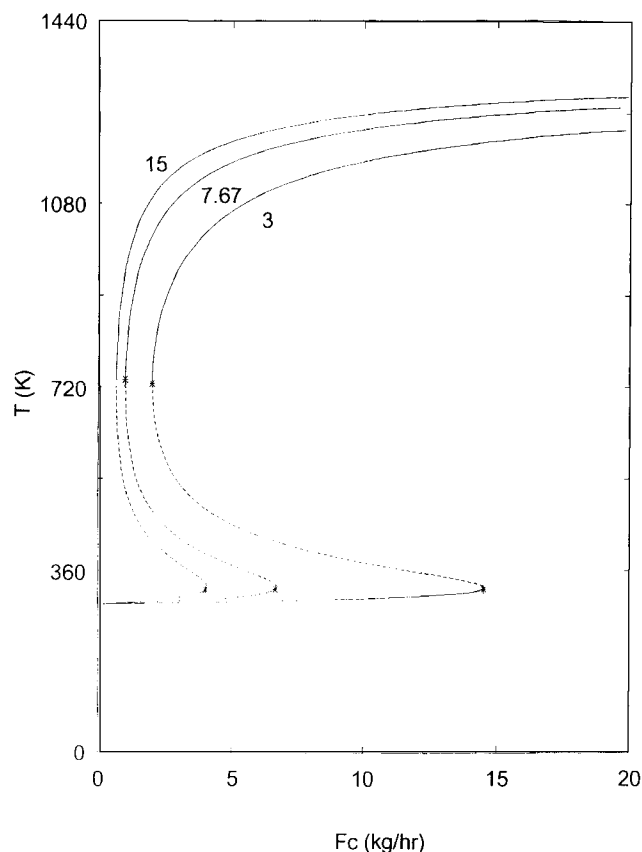


**Figure 5. Steady states and stability for the combined reactor and cooling system using an ethylene partial pressure controller ( $k_d = 0.0001 \text{ s}^{-1}$ ,  $E_a = 9,000 \text{ cal/mol}$ ).**

—, Stable steady state; ---, unstable steady state; \*, Hopf bifurcation point.

temperatures above the melting point of the polymer if catalyst feed rates are too large. Catalysts with larger activation energies are more sensitive to changes in reactor temperature, and exhibit multiple steady states. As the activation energy increases, the range of catalyst feed rates for which a high temperature steady state exists becomes larger. Although the low temperature branch of the steady-state curve is stable, disturbances in the catalyst feed rate, catalyst properties, or cooling system could lead to reactor runaway toward the high temperature steady state.

In Figure 7, multiplicity and stability information for the system is presented in a slightly different way. Activation energy is plotted as the bifurcation parameter along the abscissa, and steady-state operating temperatures are shown for several fixed-catalyst feed rates. For catalyst feed rates of 5.0 and 8.0 kg/h either a single low temperature steady state occurs or there are three steady states with the lower and upper steady states being stable and the middle steady state unstable. For intermediate catalyst feed rates of 5.8 and 7.0 kg/h, there are certain catalyst feed rates for which a single unstable steady state is observed. Limit cycle behavior is observed at these catalyst feed rates. Figure 8 summarizes the multiplicity and stability behavior from Figures 6 and 7. In region A, there is a unique unstable steady state. Region B

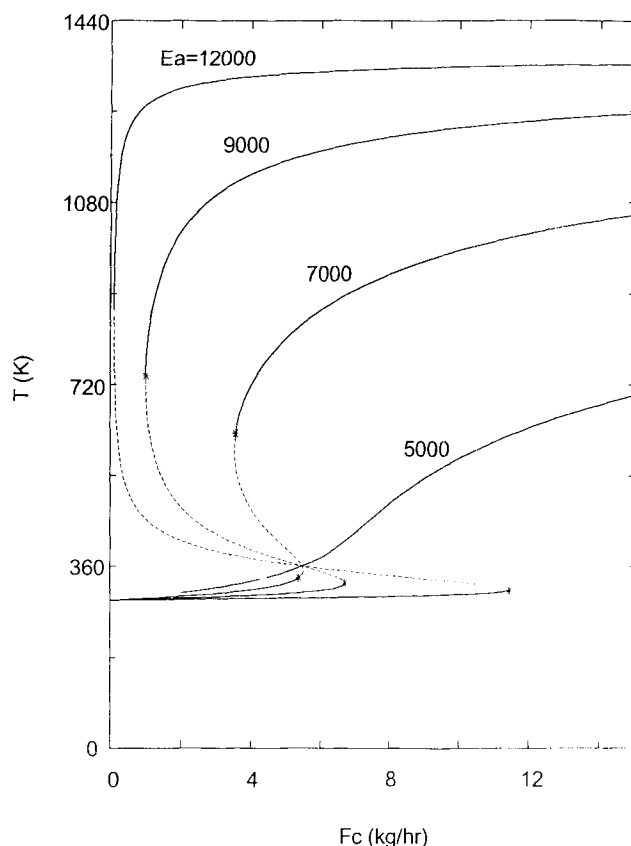


**Figure 6. Effect of activation energy on stability and multiplicity ( $k_d = 0.0001 \text{ s}^{-1}$ ,  $p_{M1sp} = 7.67 \text{ atm}$ ).**

—, Stable steady state; ---, unstable steady state; \*, Hopf bifurcation point.

has three steady states, with the upper and lower stable and the middle unstable. Region C also has three steady states, with both the middle and lower unstable and the upper stable. Regions D and E correspond to unique high temperature and low temperature steady states, respectively.

#### *Effect of heat exchanger size and operating conditions*

The area available for heat transfer,  $AU$ , and the first-order time constant,  $\tau$ , have very little effect on either the location or the stability of the steady states.  $AU$  was varied over two orders of magnitude, from  $1.14 \times 10^5$  to  $1.14 \times 10^6$ , and  $\tau$  was varied from 100 s to 3,600 s. In all cases, the steady-state curves and stability predictions were nearly coincident with the corresponding curves in Figures 5 and 6. A second-order overdamped model of the heat exchanger was also tested and had very little effect. One explanation for the insensitivity of the reactor behavior to the heat exchanger size and dynamics is that instability and multiple steady states arise due to autothermal feedback within the reactor itself.

The cooling water temperature  $T_w$  is often used as a manipulated variable for feedback control of the reactor temperature (McAuley, 1992). As expected, Figure 9 shows that the cooling water temperature has a significant effect on the steady-state reactor temperature. For the conditions simulated in Figure 9, cooling water temperatures greater than



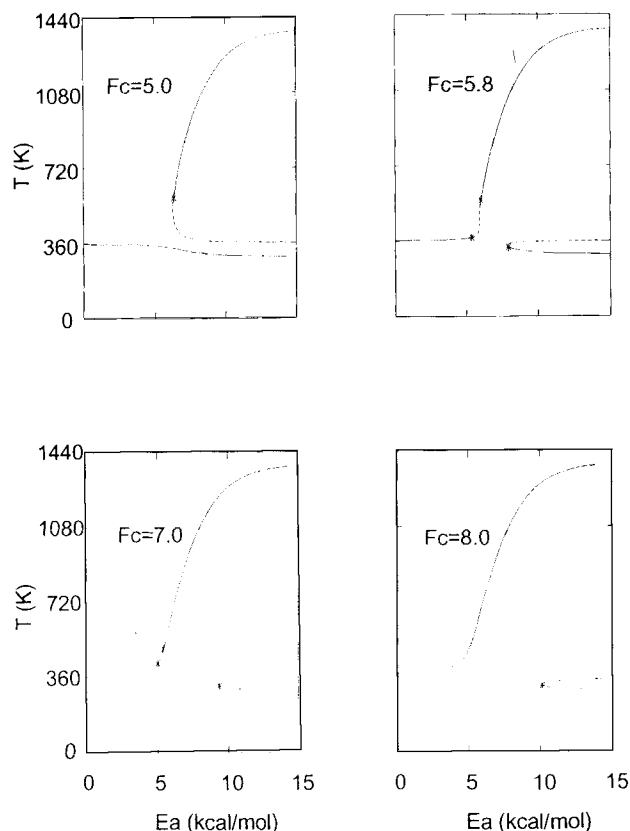


**Figure 7. Effect of catalyst feed rate on stability and multiplicity ( $k_d = 0.0001 \text{ s}^{-1}$ ,  $p_{M1sp} = 7.67 \text{ atm}$ ).**

—, Stable steady state; ---, unstable steady state; \*, Hopf bifurcation point.

298 K result in an undesirable high-temperature steady state. Even in the limit when the cooling water freezes, a high-temperature steady state exists. From Figure 9, it appears that if the reactor experiences an excursion toward a high-temperature steady state, then manipulation of the cooling water temperature alone may not be sufficient to bring the temperature back to the desired level.

#### Importance of multiple catalyst sites

The results in Figures 2 to 8 have been obtained using a catalyst with a single type of active site. In Figure 10, multiplicity and stability behavior are shown for a two-site Ziegler-Natta catalyst in which half of the sites have activation energy  $E_{a1}$  and the other half have activation energy  $E_{a2}$ . Both sites have the same deactivation rate constant,  $k_d = 0.0001 \text{ s}^{-1}$ , and the same propagation rate constant at 360 K. The ethylene partial pressure controller setpoint is 7.67 atm and the catalyst feed rate is 4.8 kg/h. The results in Figure 10 demonstrate what happens when the active sites are allowed to have different activation energies for the propagation reaction. When both activation energies are low, a unique stable low temperature steady state is observed. When both activation energies are high, a unique, stable high temperature steady state is observed. In the region between the dashed and solid lines, there is a unique, unstable steady state and the reactor experiences limit cycle behavior. If the cata-

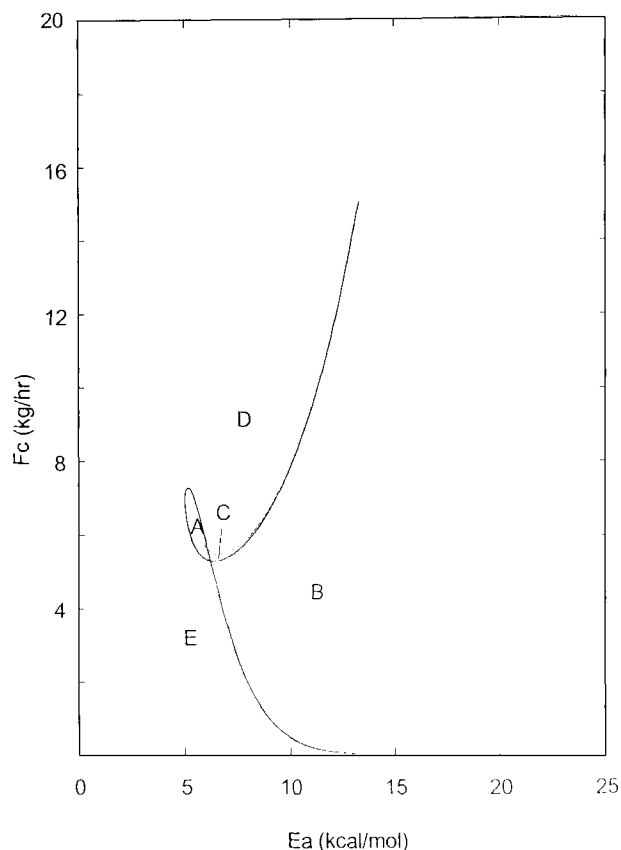


**Figure 8. Stability and multiplicity regions for the combined reactor and recycle system.**

lyst feed rate were allowed to change along a third axis, a three-dimensional bifurcation diagram could be constructed wherein Figure 10 would correspond to the plane where  $F_c = 4.8 \text{ kg/h}$  and Figure 8 would correspond to the diagonal plane where  $E_{a1} = E_{a2}$ .

#### Effect of catalyst deactivation

In Figures 2 to 10, the rate of catalyst deactivation was assumed to be independent of temperature. Figure 10 demonstrates the effect of catalyst deactivation on stability and multiplicity behavior for a single-site catalyst with an activation energy for propagation of 9,000 cal/mol. As shown in Figure 11, a catalyst with a constant deactivation rate constant of  $0.0001 \text{ s}^{-1}$  leads to an improvement in reactor stability over a nondeactivating catalyst, since the lower portion of the steady-state curve extends over a larger range of catalyst feed rates. When temperature-dependent deactivation is added to the reactor model with  $k_d = 0.0001 \text{ s}^{-1}$  at 360 K, and an activation energy for deactivation of 13,000 cal/mol, multiple steady states are not observed. However, the single steady state is open-loop, unstable for catalyst feed rates between 2.1 and 18.8 kg/h. Thus, even with a catalyst that deactivates at high temperatures, the reactor would be prone to limit cycles, which would lead to dynamic operating temperatures that are well beyond the melting temperature of the polymer particles.

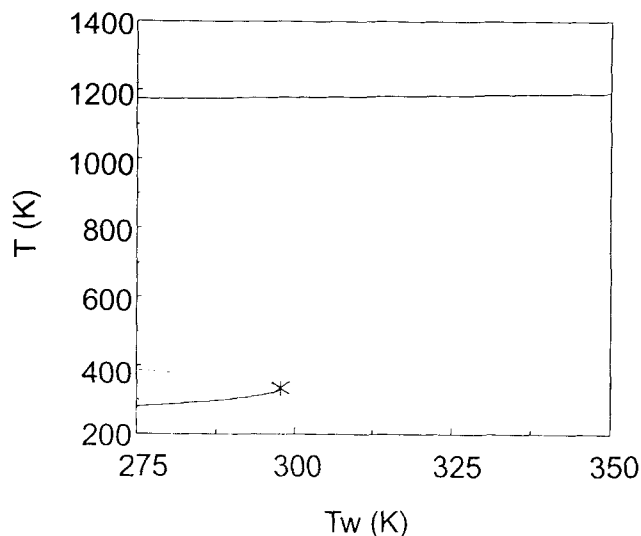


**Figure 9. Effect of cooling water temperature on steady-state operating temperature ( $k_d = 0.0001 \text{ s}^{-1}$ ,  $p_{M1sp} = 7.67 \text{ atm}$ ,  $E_a = 9,000 \text{ cal/mol}$ ,  $F_c = 5.8 \text{ kg/h}$ ).**

—, Stable steady state; ---, unstable steady state;  
\*, Hopf bifurcation point.

#### Effect of hydrogen, inerts, and comonomer

Gas-phase polyethylene reactors are operated with other components in the reactor in addition to ethylene. Nitrogen or other inerts may be added as a carrier for the catalyst or to assist in heat removal from the polymer particles. Hydrogen is added to control molecular weight. Comonomers such as butene and hexene are added to produce linear low density polyethylene copolymers. Figure 12 shows that adding nitrogen and hydrogen to the reactor at a rate of 2 mol/s has very little effect on the multiplicity and stability behavior of the reactor. In Figure 12, the ethylene partial pressure is con-

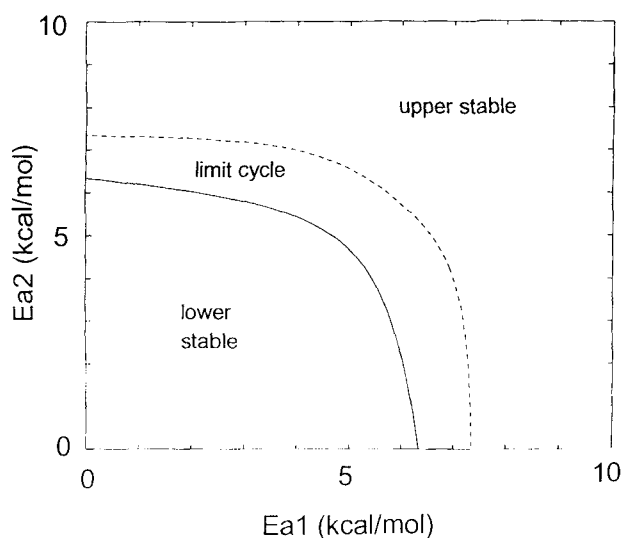


**Figure 10. Effect of activation energies of active sites on reactor stability ( $k_d = 0.0001 \text{ s}^{-1}$ ,  $p_{M1sp} = 7.67 \text{ atm}$ ,  $F_c = 4.8 \text{ kg/h}$ ).**

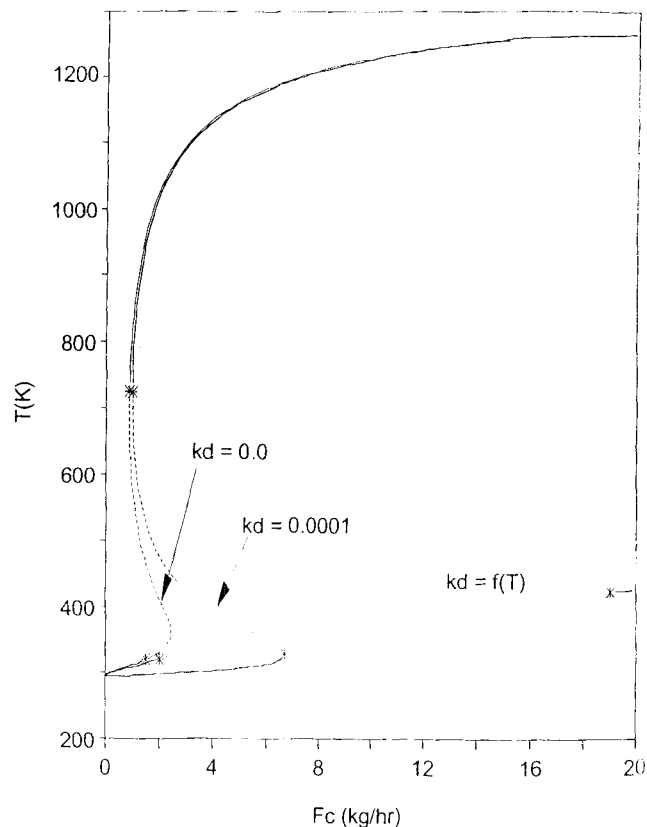


**Figure 11. Effect of catalyst deactivation on multiplicity and stability ( $p_{M1sp} = 7.67 \text{ atm}$ ,  $E_a = 9,000 \text{ cal/mol}$ ,  $F_c = 5.8 \text{ kg/h}$ ).**

—, Stable steady state; ---, unstable steady state;  
\*, Hopf bifurcation point.

trolled at 7.67 atm and  $k_d = 0$ . Compared with the  $k_d = 0$  case in Figure 10, there is very little change in the steady-state behavior. Slight differences are caused by the different heat capacities of the gases, and by the deactivating influence of hydrogen on the catalyst (Eq. 18).

Figure 12 shows the effect of butene addition to the reactor using a catalyst with  $k_d = 0.0001 \text{ s}^{-1}$  and  $E_a = 9,000 \text{ cal/mol}$ . The comonomer has a very mild effect on the reactor operation for the propagation rate constants given in Table 2, but does not significantly alter the multiplicity and stability behavior of the reactor system. Butene is consumed to a much smaller extent than ethylene, so the reactor behavior is far more sensitive to the ethylene concentration than the butene concentration.

#### Conclusions

A gas-phase ethylene polymerization model has been analyzed to determine the effects of reactor operating conditions on dynamics and stability. The reactor model employed assumed that both the gas and polymer phases in the reactor are well mixed. Our analysis of ethylene homopolymerization in the reactor alone gives similar results to those of Choi and Ray (1985b), confirming that mass- and heat-transfer limitations between multiple phases are not responsible for the observed bifurcation behavior.

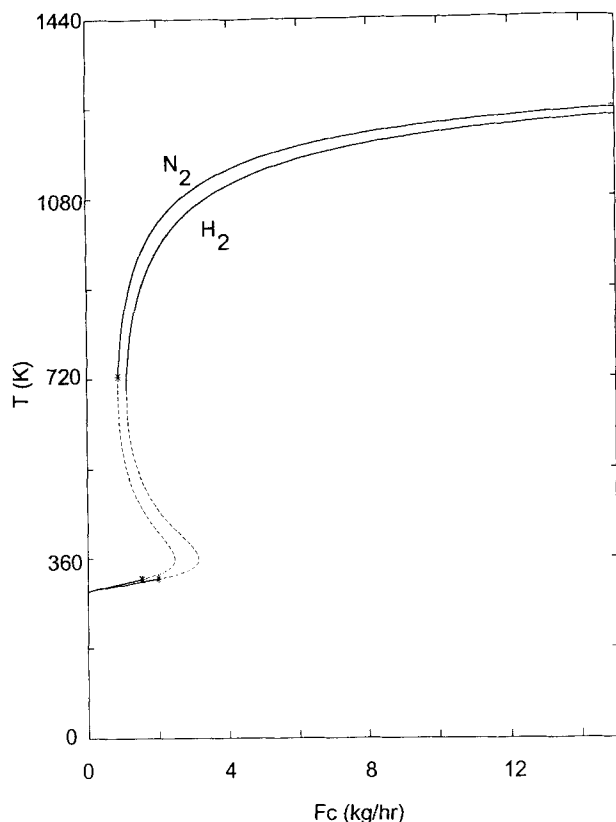


**Figure 12. Effect of nitrogen and hydrogen on stability and multiplicity.**

—, Stable steady state; ---, unstable steady state; \*, Hopf bifurcation point.

The reactor model was extended to account for the effects of the external heat exchanger and the recycle stream. Accounting for the recycle stream is important because the recycle to fresh feed ratio in gas-phase polyethylene reactors is on the order of 50 to 1 (Xie et al., 1994). The combined system was shown to exhibit unstable behavior and limit cycles. Because the unstable behavior arises due to positive feedback between the reactor temperature and polymerization rate, the size and dynamics of the heat exchanger have very little effect on either the stability or multiplicity of the system.

It was shown that the presence of an ethylene partial-pressure controller had a significant effect on multiplicity and stability. Higher partial-pressure setpoints made the reactor more prone to run away toward undesirable high temperature steady states by ensuring that ample monomer is always available for the reaction. The catalyst feed rate, activation energy, and deactivation properties were also shown to have a significant influence on reactor behavior. If a multiple-site catalyst is used for the polymerization, then both the distribution and kinetic behavior of the individual sites on the catalyst can affect the dynamic behavior and stability of the system. Hydrogen, inert components, and butene comonomer were shown to have only a very minor effect on system behavior.

The results in this study demonstrate that without feed-

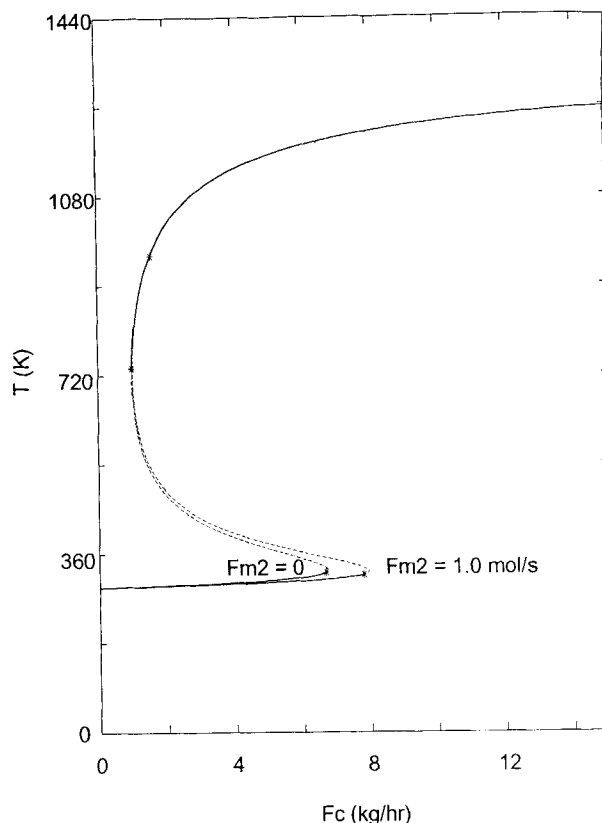


**Figure 13. Effect of butene comonomer on stability and multiplicity.**

—, Stable steady state; ---, unstable steady state; \*, Hopf bifurcation point.

back temperature control, gas-phase polyethylene reactors are prone to unstable steady states, limit cycles, and excursions toward unacceptably high temperature steady states. Minor design changes to the external heat exchanger cannot be used to ensure open-loop stability, so feedback temperature control is very important in gas-phase polyethylene reactors. Without feedback temperature control, disturbances in the catalyst feed rate, catalyst properties, or ethylene concentration in the reactor could cause the system to move away from a desirable steady state into an unacceptable operating regime. Such information about the underlying properties of the system is very important to the design of reactor operating policies and to the implementation of stabilizing feedback temperature controllers.

## Acknowledgment

The authors thank the Principal's Development Fund of Queen's University and the Natural Science and Engineering Research Council of Canada for support of this research.

## Notation

$K$  = ethylene partial-pressure controller gain  
 $p_i$  = partial pressure of component  $i$   
 $R_i$  = rate of consumption of component  $i$  by reaction  
 $t$  = time

$Y_1, Y_2$  = quantity of active catalyst sites of type 1 and type 2, respectively [mol]

## Greek letters

$\gamma$  = dimensionless group defined in Eq. 17

$\tau_i$  = integral time for ethylene partial-pressure controller

## Subscripts

0 = reactor inlet condition

1, M1 = ethylene

2, M2 = butene comonomer

$f$  = fresh feed stream

$g0$  = gas recycle stream entering the reactor

$I$  = inert component

$r$  = due to reaction

$ss$  = steady state

$top$  = condition of stream leaving the top of the reactor

$w$  = cooling water

$Y_i$  = catalyst site of type  $i$

## Literature Cited

- Adebekun, A. K., K. M. Kwalik, and F. J. Schork, "Steady-State Multiplicity During Solution Polymerization of Methyl Methacrylate in a CSTR," *Chem. Eng. Sci.*, **44**(10), 2269 (1989).
- Choi, K. Y., and W. H. Ray, "Recent Developments in Transition Metal Catalyzed Olefin Polymerization—A Survey I. Ethylene Polymerization," *J. Macromol. Sci. Rev. Macromol. Chem. Phys.*, **C25**, 1 (1985a).
- Choi, K. Y., and W. H. Ray, "The Dynamic Behavior of Fluidized Bed Reactors for Solid Catalyzed Gas Phase Olefin Polymerization," *Chem. Eng. Sci.*, **41**(12), 2261 (1985b).
- Choi, K. Y., and W. H. Ray, "The Dynamic Behavior of Continuous Stirred-Bed Reactors for the Solid Catalyzed Gas Phase Polymerization of Propylene," *Chem. Eng. Sci.*, **43**(10), 2587 (1988).
- Doedel, E. J., "AUTO: Software for Continuation and Bifurcation Problems in Ordinary Differential Equations," California Institute of Technology, Pasadena, CA (1986).
- Hamer, J. W., T. A. Akramov, and W. H. Ray, "The Dynamic Behavior of Continuous Polymerization Reactors—II. Nonisothermal Solution Homopolymerization and Copolymerization in a CSTR," *Chem. Eng. Sci.*, **36**, 1897 (1981).
- Hutchinson, R. A., and W. H. Ray, "Polymerization of Olefins through Heterogeneous Catalysis. VII. Particle Ignition and Extinction Phenomena," *J. Appl. Poly. Sci.*, **34**, 657 (1987).
- Hutchinson, R. A., and W. H. Ray, "Polymerization of Olefins through Heterogeneous Catalysis—The Effect of Condensation Cooling on Particle Ignition," *J. Appl. Poly. Sci.*, **43**, 1387 (1991).
- Jaisinghani, R., and W. H. Ray, "On the Dynamic Behavior of a Class of Homogeneous Continuous Stirred Tank Polymerization Reactors," *Chem. Eng. Sci.*, **32**, 811 (1977).
- Lovo, M., and V. Balakotaiah, "Multiplicity Features of Adiabatic Autothermal Reactors," *AIChE J.*, **38**(1), 101 (1992).
- McAuley, K. B., "Modelling, Estimation and Control of Product Properties in a Gas Phase Polyethylene Reactor," PhD Thesis, McMaster Univ., Hamilton, Ont., Canada (1992).
- McAuley, K. B., and J. F. MacGregor, "On-Line Inference of Polymer Properties in an Industrial Polyethylene Reactor," *AIChE J.*, **37**(6), 825 (1991).
- McAuley, K. B., and J. F. MacGregor, "Optimal Grade Transitions in a Gas Phase Polyethylene Reactor," *AIChE J.*, **38**, 1564 (1992).
- McAuley, K. B., and J. F. MacGregor, "Nonlinear Product Property Control in Industrial Gas Phase Polyethylene Reactors," *AIChE J.*, **39**(5), 855 (1993).
- McAuley, K. B., J. F. MacGregor, and A. E. Hamielec, "A Kinetic Model for Industrial Gas Phase Ethylene Copolymerization," *AIChE J.*, **36**(6), 837 (1990).
- McAuley, K. B., J. P. Talbot, and T. J. Harris, "A Comparison of Two-Phase and Well-Mixed Models for Fluidized Bed Polyethylene Reactors," *Chem. Eng. Sci.*, **49**(13), 2035 (1994).
- Morbidelli, M., A. Varma, and R. Aris, "Reactor Steady-State Multiplicity and Stability," *Chemical and Reaction Engineering*, Chap. 15, J. J. Carberry and A. Varma, eds., Marcel Dekker, New York (1987).
- Rawlings, J. B., "Simulation and Stability of Continuous Emulsion Polymerization Reactors," PhD Thesis, Univ. of Wisconsin, Madison (1985).
- Razon, L. F., and R. A. Schmitz, "Multiplicities and Instabilities in Chemically Reacting Systems—A Review," *Chem. Eng. Sci.*, **42**(5), 1005 (1987).
- Schmidt, A. D., and W. H. Ray, "The Dynamic Behavior of Continuous Polymerization Reactors: I. Isothermal Solution Polymerization in a CSTR," *Chem. Eng. Sci.*, **36**, 1401 (1981).
- Schmidt, A. D., A. B. Clinch, and W. H. Ray, "The Dynamic Behavior of Continuous Polymerization Reactors: III. An Experimental Study of Multiple Steady States in Solution Polymerization," *Chem. Eng. Sci.*, **39**(3), 419 (1984).
- Talbot, J. P., "The Dynamic Modelling and Particle Effects on a Fluidised Bed Polyethylene Reactor," PhD Thesis, Queen's Univ., Kingston, Ont., Canada (1990).
- Teymour, F., and W. H. Ray, "The Dynamic Behavior of Continuous Solution Polymerization Reactors: IV. Dynamic Stability and Bifurcation Analysis of an Experimental Reactor," *Chem. Eng. Sci.*, **44**(9), 1967 (1989).
- Teymour, F., and W. H. Ray, "The Dynamic Behavior of Continuous Polymerization Reactors: V. Experimental Investigation of Limit-Cycle Behavior for Vinyl Acetate Polymerization," *Chem. Eng. Sci.*, **47**(15/16), 4121 (1992a).
- Teymour, F., and W. H. Ray, "The Dynamic Behavior of Continuous Polymerization Reactors: VI. Complex Dynamics in Full-Scale Reactors," *Chem. Eng. Sci.*, **47**(15/16), 4133 (1992b).
- Uppal, A., W. H. Ray, and A. B. Poore, "On the Dynamic Behavior of Continuous Stirred Tank Reactors," *Chem. Eng. Sci.*, **29**, 967 (1974).
- Uppal, A., W. H. Ray, and A. B. Poore, "The Classification of the Dynamic Behavior of Continuous Stirred Tank Reactors—Influence of Reactor Residence Time," *Chem. Eng. Sci.*, **31**, 205 (1976).
- Van Heerden, C., "Auto thermic Processes: Properties and Reactor Design," *Ind. Eng. Chem.*, **45**, 1242 (1953).
- Xie, T., K. B. McAuley, C. C. Hsu, and D. W. Bacon, "Gas Phase Ethylene Polymerization: Production Processes, Polymer Properties, and Reactor Modelling," *Ind. Eng. Chem. Res.*, **33**(3), 449 (1994).

Manuscript received Nov. 29, 1993, and revision received Apr. 22, 1994.